INTERNATIONAL JOURNAL OF OPTIMIZATION IN CIVIL ENGINEERING
Int. J. Optim. Civil Eng., 2020; 10(4):651-668

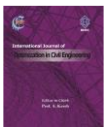

PERFORMANCE-BASED LAYOUT OPTIMIZATION FOR BRACED STEEL FRAMES USING FINITE DIFFERENCE ALGORITHM

M. Danesh[*, †] and A. Iraji
Department of Civil Engineering, Urmia University, Urmia, Iran

ABSTRACT

The efficiency of braced structures depends significantly on structure response under seismic loads. The main design challenge for these type of structures is to select shape, number of spans, and type of connections appropriately. Therefore, introducing an optimized and cost-effective design including a certain level of safety and performance against natural hazards seems to be an inevitable necessity. The present work introduces a performance-based design for braced steel structures as well as an optimized arrangement of braces and connection types via using finite difference algorithm. The results show that the latter two factors are very important and necessary to achieve an optimized design for braced steel structures.

Keywords: discrete optimization; braced steel frame; performance-based design; finite difference algorithm; layout optimization.

Received: 5 September 2020; Accepted: 10 November 2020

1. INTRODUCTION

Structural design should meet the rules of the present codes to be considered as safe design and sustain the expected loads. Engineers always have a challenge in structural design. It is to design a cost-effective structure. There is another challenge in which engineers have to meet the rules of the design codes simultaneously cost-effective. The experience of the designer as well as the procedure of trial and error during a design job can help the engineer to perform the structural design properly. Doing a good optimized design in seismic regions can be a difficult and time-consuming job [1]. In addition to this, doing a most optimized

[*]Corresponding author: Department of Civil Engineering, Urmia University, Urmia, P.O. box 165, Iran
[†]E-mail address: m.danesh@urmia.ac.ir (M. Danesh)

design is another challenge. The need to reach a most cost-effective design caused many developments in this field.

Northridge earthquake with magnitude of 6.7 Mw caused damage at 20 billion dollars in 1994. After this earthquake Structural Engineers Association of California (SEAOC) seriously recommended the new method for structural seismic design, which uses performance-based design framework. SEAOC recommends the performance-based design method instead of the traditional force-based design. The performance-based method considers the plastic behavior of the structures during strong motions. The total cost of the building can also be evaluated during the usable life of the structure [2]. SEAOC introduced the concept of the seismic performance-based design in 1995. Based on this definition, it is necessary to satisfy some special rules to achieve target performance in different performance and hazard levels [3]. Different collapse levels are defined based on the structure nonlinear displacements in this method under strong motions . James et al. [4] introduced an early study in this field. They proposed a performance-based optimization design method. Ganzerli et al. [5] combined the present concept of performance-based design method with the optimization methods. They proposed a nonlinear analysis method in which some performance-based constraints were introduced based on the recommended plastic hinges by FEMA-356 [6] for the members Zou and Chan [7] introduced an optimization method based on the concept of optimality criterion. They defined the nonlinear response of moment frames based on the design variables using virtual work method and Tailor series. They calculated inelastic inter-story drifts using pushover analysis method. Therefore, the effect of higher modes has not been considered.

PBD is one of the deterministic design methods that do not consider uncertainties; therefore, it cannot evaluate the probability of damages and collapse satisfactorily.

The performance-based optimization is a seismic design method based on the combination of performance and optimization. The selection of the braces location and type of connections is one of the most important aspects of this design procedure. This selection is performed usually based on the available experiences which is not cost-effective in most times. Because of high degree of indeterminacy in structures, a minor change in shape of the structures leads to high variations in internal forces and cross section areas of the structure members.

Gholizadeh et al. [8] investigated the optimization of braces location for braced steel frames using dolphin meta-heuristic algorithm. They studied several steel frames with different stories in which the location of braces was optimized. This optimization decreased 10% of the total weight of steel materials.

Kaveh et al. [9] investigated different steel frames with 5 spans and different story numbers using different algorithms. They ignored the irregularities of the structures. They used linear static analysis method to evaluate the structure response. Different x-brace layouts were introduced in this study.

Ohsaki and Hagishita [10] studied to find an appropriate brace layout optimization and brace type. The studied structure had five spans and three stories. The results showed that the appropriate brace type was dependent on its position. They showed that the placement of X-bracing at lower stories and K- and V-bracings at higher stories is more cost-effective.

Farzampour et al [11] optimized Butterfly-shaped shear links at single story steel frames with a single bay geometrically via using grey wolf algorithm and achieved most cost

effective dimensions for that.

Mansouri et al [12] performed the weight-optimization for two four-bay dual frames with X-bracings and five and nine stories via using Bee colony algorithm. They concluded that the LS performance is predominant for two types of frames.

Mirzayi et al [13] used two algorithms of Gravity search algorithm and Particle swarm optimization to optimize tuned mass dampers for two ten- and forty-story frames with shear wall. They could evaluate the uniformity and calculate the reduced values of Inter-story drifts.

Terazawa and Takeuch [14] introduced an optimized design method of dampers for braced frames on the base of generalizing response spectrum analysis. They evaluated the geometry of the damper and found its optimized location for a 3D nine-story steel frame via using genetic algorithm and Particle swarm optimization methods.

Kaveh et al [15] optimized the location of braces for braced three-, six-, and nine-story steel frames via using colliding bodies optimization, Particle swarm optimization, imperialist competitive algorithm, and modified dolphin monitoring operator methods and compared the results with each other.

The used FDA optimization algorithm in this paper was originally introduced by authors in reference [16]. This paper presents the capability of the introduced method in optimizing the X-bracings layout for dual systems. The verification of this method has been performed previously in this reference and the details can be found there.

The purpose of the present study is layout optimization of steel braced frames with X-bracings. Because of the complexity of this type of optimization, it is necessary to develop an efficient algorithm. The FDA meta-heuristic algorithm (Finite Difference Algorithm) introduced by authors [16] was employed in the present research. The position and type of connections were implemented in addition to the positions of X-bracings in this method. The technical literature in the field of Finite Difference Algorithm will be discussed in the next section.

2. FINITE DIFFERENCE ALGORITHM

X^* can be considered as a minimum answer when $f'(X^*)=0$ and $f''(X^*)>0$ for the equation $y=f(x)$. Therefore, root of the equation $f'(x)=0$, can be an optimum value for the equation $y=f(x)$. Most of the civil engineering problems have not explicit functions. Moreover, they consist of several dependent variables that lead to very difficult solutions. Note that if the target function is explicit, the possibility of calculation of gradient and hessian will be so difficult and not possible in some cases. The FDA meta-heuristic algorithm was extracted from the Newton-Raphson method to find the roots of nonlinear equations. This algorithm is exerted on the target function of optimization and the population is assumed as a single variable without considering its dimensions. This algorithm then finds the optimized point of target function via solution of the nonlinear equation, $\Phi'(X) = 0$, and using the Newton-Raphson method. This algorithm is a nonlinear meta-heuristic type based on the population and without using the natural phenomena and can be used to solve continuous or discrete and constraint or non-constraint optimization problems. Fig. 1 shows the concept of this algorithm.

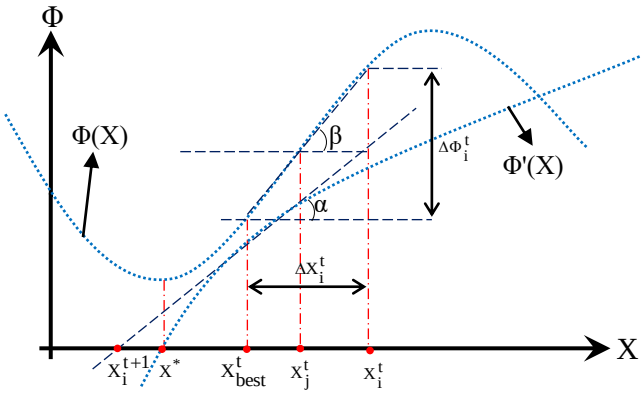

Figure 1. Newton- Raphson method to find roots of nonlinear equation Φ'(X)=0

3. MATHEMATICAL MODEL OF ALGORITHM

The Newton-Raphson method can be introduced as an iteration way to find the root of equation $f'(x) = 0$ as follows:

$$x_i^{t+1} = x_i^t - \frac{f'(x_i^t)}{f''(x_i^t)} \tag{1}$$

Consider x_{i-1}, x_i, and x_{i+1} three sequential variables of the population with the assumption of $f(x_{i+1})>f(x_i)>f(x_{i-1})$; therefore:

$$\begin{cases} x_i - x_{i-1} = \kappa(x_{i+1} - x_{i-1}) \\ \\ x_{i+1} - x_i = (1-\kappa)\times(x_{i+1} - x_{i-1}) \end{cases} \quad ,\kappa < 1 \tag{2}$$

Assume $f(x_{i-1})=f_{i-1}$, $f(x_i)=f_i$, & $f(x_{i+1})=f_{i+1}$; let α be the slope of the line between two points x_{i-1} and x_{i+1}, and β the slope of the tangent line to the curve f:

$$\alpha \approx \beta \rightarrow \begin{cases} f'_i = \dfrac{f_{i+1} - f_{i-1}}{x_{i+1} - x_{i-1}} \\ \\ f''_i = \dfrac{f'_i - f'_{i-1}}{x_{i+1} - x_{i-1}} \end{cases} \tag{3}$$

$$\rightarrow f''_i = \frac{\dfrac{f_{i+1} - f_i}{(1-\kappa)(x_{i+1} - x_{i-1})} - \dfrac{f_i - f_{i-1}}{\kappa(x_{i+1} - x_{i-1})}}{x_{i+1} - x_{i-1}} = \frac{1}{\kappa(1-\kappa)} \frac{\kappa f_{i+1} - f_i + (1-\kappa) f_{i-1}}{(x_{i+1} - x_{i-1})^2} \tag{4}$$

Equations (3) and (4) are replaced in Equation (1) as follows:

$$x_i^{t+1} = x_i^t - \frac{\frac{f_{i+1}^t - f_{i-1}^t}{x_{i+1}^t - x_{i-1}^t}}{\frac{1}{\kappa(1-\kappa)}\frac{\kappa f_{i+1}^t - f_i^t + (1-\kappa) f_{i-1}^t}{\left(x_{i+1}^t - x_{i-1}^t\right)^2}} = x_i^t - \kappa(1-\kappa)\frac{f_{i+1}^t - f_{i-1}^t}{\kappa f_{i+1}^t - f_i^t + (1-\kappa) f_{i-1}^t}\left(x_{i+1}^t - x_{i-1}^t\right) \tag{5}$$

$$grad_i^{t+1} = \kappa(1-\kappa)\frac{f_{i+1}^t - f_{i-1}^t}{\kappa f_{i+1}^t - f_i^t + (1-\kappa) f_{i-1}^t} \tag{6}$$

$$x_i^{t+1} = x_i^t - grad_i^{t+1} \times \left(x_{i+1}^t - x_{i-1}^t\right) \tag{7}$$

Equation (7) uses exploitation to find the optimized function point. However, to prevent finding only the local optimized point and giving it an exploration to the solution, a weight ratio of the current iteration number (*CurrItr*) to the total iteration number (*TotItr*) is used and equation (7) is re-formulated as follows:

$$x_i^{t+1} = x_i^t - r \otimes grad_i^{t+1}\left(1 - \frac{CurrItr}{TotItr}\right) \times \left(x_{i+1}^t - x_{i-1}^t\right) - \frac{CurrItr}{TotItr}\left(x_i^t - x_{i-1}^t\right) \tag{8}$$

where, *r* is a random vector whose arrays number equals the variables number of *f*, and is at the range of (0,1) with a uniform distribution, and $\otimes$ is array-to-array multiplication.

4. EVALUATING STRUCTURE DEMAND AND RESPONSE

4.1 Force-based design constraints

Geometrical constraints of the connections are formulated using Fig. 2 as follows:

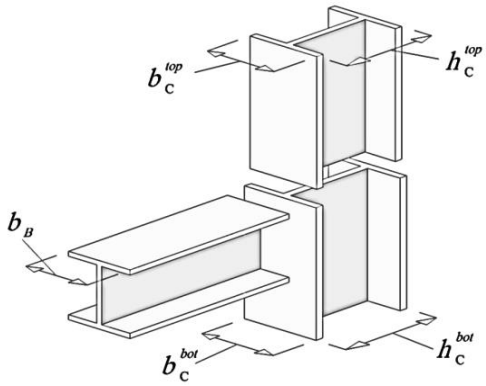

Figure 2. Dimensions of beams and columns cross-sections at connections

$$g_{able}(x)=\begin{cases}\left(\dfrac{h_c^{top}}{h_c^{bot}}\right)_i-1\le 0\\ \left(\dfrac{b_c^{top}}{b_c^{bot}}\right)_i-1\le 0,\quad i=1,2,\ldots,n_e\\ \left(\dfrac{b_b}{b_c^{bot}}\right)_i-1\le 0\end{cases} \tag{9}$$

The geometrical constraints mentioned in Equation (9) are checked and satisfied, and then design constraints including limit states and serviceability under gravitational load combinations are checked. Gravitational load combinations are applied using AISC-LRFD [17] code as follows:

Q_D and Q_L are dead and live loads, respectively. The constraints are checked for all non-seismic load combinations for all structural members as follows:

$$Q_G^{FBD}=\begin{cases}1.4Q_D\\ 1.2Q_D+1.6Q_L\end{cases} \tag{10}$$

$$g_{FBD}(x)=\begin{cases}\left[\dfrac{P_u}{2\phi_c P_n}+\left(\dfrac{M_{ux}}{\phi_b M_{nx}}+\dfrac{M_{uy}}{\phi_b M_{ny}}\right)\right]_i-1\le 0;\quad \dfrac{P_u}{\phi_c P_n}<0.2\\ \left[\dfrac{P_u}{\phi_c P_n}+\dfrac{8}{9}\left(\dfrac{M_{ux}}{\phi_b M_{nx}}+\dfrac{M_{uy}}{\phi_b M_{ny}}\right)\right]_i-1\le 0;\quad \dfrac{P_u}{\phi_c P_n}\ge 0.2\end{cases} \tag{11}$$

where, P_u is required tension or compression strength, P_n is nominal axial strength for tension or compression, Φ_c is resistance reduction factor which is 0.9 for tension and 0.85 for compression, M_{ux} and M_{uy} are required flexural strengths in x and y directions, respectively, M_{nx} and M_{ny} are nominal flexural strength in x and y directions, respectively, Φ_b is flexural resistance reduction factor which is 0.9 and n_e is number of elements.

Because the seismic loads determine the limit state for lateral displacements, therefore this is done in the case of performance-based design and is ignored in the case of force-based design. In order to decrease the amount of calculations, each member of the population is considered in the procedure of the optimization if only to satisfy the related constraints, otherwise, it is not considered with the selection of an appropriate penalty coefficient.

4.2 Performance-based design constraints

The lateral displacement of a building may damage mechanical and electrical facilities, cause falling of attached components to the ceiling, and provide discomfort for the building

inhabitants. The concept of the PBD method is actually based on the displacement in which the design and capacity criteria are evaluated based on the displacement [18]. Inter-story drifts at different performance levels are calculated using nonlinear static analysis. Gravity loads are chosen using FEMA-356 [6] as follows:

$$Q_G^{PBD} = 1.1(Q_D + Q_L) \tag{12}$$

Response spectrum of Iranian standard 2800 [19] at the level of design earthquake with the occurrence probability of 10% during 50 years is employed to calculate spectrum acceleration, S_a, at three performance levels, Immediate occupancy (IO), life safety (LF), and collapse prevention (CP). The resulting acceleration was scaled for probabilities of 50% and 2% during 50 years at performance levels of IO and CP. Assume a building with high importance constructed in a region with very high seismic risk and on a soil deposit type II. The spectrum acceleration, S_a, is calculated as follows:

$$S_a^{10\%/50\,years} = ABI \tag{13}$$

$$B_1 = \begin{cases} S_0 + (S - S_0 + 1)\dfrac{T_e}{T_0} = 1.1 + 11T & ;\ 0 < T_e < 0.15s \\ S + 1 = 2.75 & ;\ 0.15 < T_e < 0.7s \\ (S+1)\dfrac{T_s}{T_e} = \dfrac{1.925}{T_e} & ;\ T_e > 0.7s \end{cases} \tag{14}$$

$$B = B_1 N \tag{15}$$

$$N = \begin{cases} 1 & ;\ T_e < 0.7s \\ \dfrac{0.7}{4 - T_s}(T_e - T_s) + 1 = \dfrac{7}{33}(T_e - 0.7) + 1 & ;\ 0.7 < T_e < 4s \\ 1.7 & ;\ T_e > 4s \end{cases} \tag{16}$$

$$S_a^{50\%/50years} = S_a^{10\%/50years}\left(\frac{75}{475}\right)^{0.44} \approx 0.4439\, S_a^{10\%/50years} \tag{17}$$

$$S_a^{2\%/50years} = S_a^{10\%/50years}\left(\frac{2475}{475}\right)^{0.29} \approx 1.5 S_a^{10\%/50years} \tag{18}$$

where, A is the ratio of structure acceleration to gravity acceleration, B is the coefficient of structure response, B_1 is base response coefficient, N is spectrum modification coefficient, I is importance coefficient, $S_a^{50\%/50years}$, $S_a^{10\%/50years}$, and $S_a^{2\%/50years}$ are spectrum accelerations corresponding to performance levels of IO, LS, CP, respectively, and T_e is the effective fundamental period of the building that can be calculated based on fundamental period and using two linearization of capacity curve method as follows:

$$T_e = T_1\sqrt{\frac{K}{K_e}} \tag{19}$$

where, K and K_e are lateral elastic stiffness and lateral effective stiffness, respectively and T_1 is the main period of the structure. The latter parameter can be achieved by two linearization of capacity curve. After calculating target displacement, we have the equation as follows:

$$\delta_t^i = C_0 C_1 C_2 C_3 S_a^i \left(\frac{T_e}{2\pi}\right)^2 g; \quad i=IO,LS,CP \tag{20}$$

where, C_0 relates the spectral displacement to the likely building roof displacement, C_1 relates the expected maximum inelastic displacements to the displacements calculated for linear elastic response, C_2 represents the effect of the hysteresis shape on the maximum displacement response and C_3 accounts for P-Δ effects.

The nonlinear static analysis is conducted and maximum inter-story drifts at performance levels of IO (θ_{IO}), LS (θ_{LS}), and CP (θ_{CP}) are calculated. Then, the constraints of the performance-based optimization can be formulated using FEMA-356 [6] as follows:

$$g_{PBD}(x) = \begin{cases} \dfrac{\theta_{IO}}{0.005} - 1 \le 0 \\ \dfrac{\theta_{LS}}{0.015} - 1 \le 0 \\ \dfrac{\theta_{CP}}{0.02} - 1 \le 0 \end{cases} \tag{21}$$

4.3 Quasi-objective function

The primary cost of steel frames is dependent on the amount of steel material. Therefore, the quasi-objective function is defined based on sequential unconstrained minimization technique (SUMT) and using exterior penalty function method (EPFM) [20] to control design constraints as follows:

$$\Phi(X) = \sum_{i=1}^{n_m} \rho_i A_i \sum_{j=1}^{n_m} L_j \left(1 + r_p \sum_{k=1}^{n_c} \left(\max\{0, g_k\}\right)\right)^2; \quad k=able,FBD,PBD \tag{22}$$

where, ρ_i is density, A_i is cross section area of the i^{th} population, n_m is the number of i^{th} population member, L_j is the length of the j^{th} member in i^{th} population, $g_k(X)$ is the k^{th} behavioral constraint, n_c is the number of constraints, r_p is the increasing penalty parameter.

5. SIMULATION

The studied models are three five-span frames with 6, 9, and 12 stories. The spans length was 6m and stories height was 3.2 m. The columns, beams and bracings were categorized at two groups at each story including internal and marginal members and at each three stories. The sections were chosen from the standard W-section category. The yield stresses of beams

and columns were assumed F_y=351.53MPa and F_y=253.1MPa, respectively, and corresponding strain hardening was 3%. The yield stress of bracings and corresponding strain hardening were assumed F_y=253.1MPa and zero, respectively. Young modulus of all steel members was E=203893.6MPa. Dead and live loads were assumed 25kN/m^2 and 15kN/m^2, respectively.

The numerical simulation was conducted via using OpenSees [21] and optimization calculations were conducted using MATLAB [22]. The elastic element of elasticBeamColumn was employed in linear simulation of beam and column elements. The nonlinearBeamColumn element was used in nonlinear simulation.

The introduced model by Jain and Goal [23] confirmed by FEMA-274 was used for non-elastic modeling of bracings. The assumed behavior was illustrated in Fig. 3. As can be seen, the post-buckling compressive strength is 20% of buckling force.

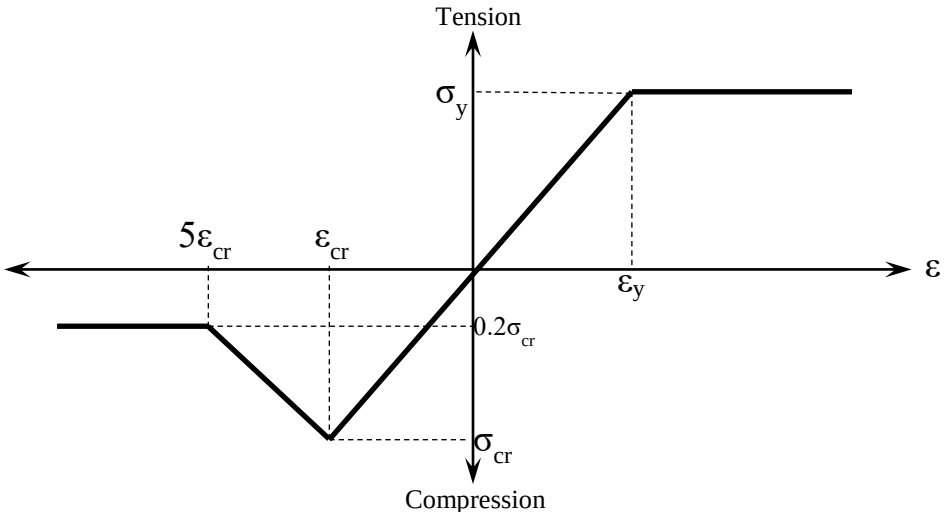

Figure 3. Assumed stress-strain behavior for bracing

6. MODELS EVALUATION

6.1 Design variables

No.	Span					Column										
	1	2	3	4	5	1	2	3	4	5	1	2	3	4	5	6
1	—	—	—	—	—	X	□	□	□	X	▲	▯	▯	▯	▯	▲
2	—	○–○	○–○	○–○	—	□	X	□	X	□	▲	▲	▯	▯	▲	▲
3	—	—	○–○	—	—	□	□	X	□	□	▲	▲	▲	▲	▲	▲
4	○–○	○–○	○–○	○–○	○–○	X	X	□	X	X	▯	▯	▯	▯	▯	▯
5	○–○	—	○–○	—	○–○	X	□	X	□	X	▯	▯	▲	▲	▯	▯
6	○–○	—	—	—	○–○	□	X	X	X	□	▯	▲	▯	▯	▲	▯
7	—	○–○	—	○–○	—	X	X	X	X	X	▯	▲	▲	▲	▲	▯
8	○–○	○–○	—	○–○	○–○						▲	▯	▲	▲	▯	▲

Figure 4. Layout of x-bracings, beam-column connections, and column to base connections

Given the number of frames' spans, considering construction related problems, and maintaining the structure symmetry, seven locations of X-bracings, eight possible symmetric layouts for column to support connections and beam to column connections were considered according to Fig. 4.

Symbols — and ○–○ indicate the beam fixed at both ends and simply supported at both ends, respectively; X and □ indicate existence or not existence of bracing, respectively; ▯ and ▲ indicate fixed column base and pinned column base, respectively.

6.2 Six-story frame

Fig. 5 shows optimized configuration of X-bracings and connections for six-story frame. Table 1 compares the resulted sections and structure weight for six-story frame at the present work with the results for dual system and building frame system by Gholizadeh, and Poorhoseini [8]. As can be seen, the resulted structure weight for the present research is lower than that of Gholizadeh, and Poorhoseini [8]. Figs. 7 and 8 show inter-story drifts for six-story frame at different performance levels and pushover curve, respectively. As seen, inter-story drifts of IO performance level are close to allowable values and the inter-story drifts for LS and CP performance levels are so far from the allowable values i.e. 1.5% and 2.0%, respectively.
Fig. 9 shows the response of the structure at different performance levels, critical design criteria at the IO performance level, axial displacements of X-bracings, and inter-story drifts. It can be seen that at the CP performance level, plastic rotation of the members are critical due to the increase in structure displacements.

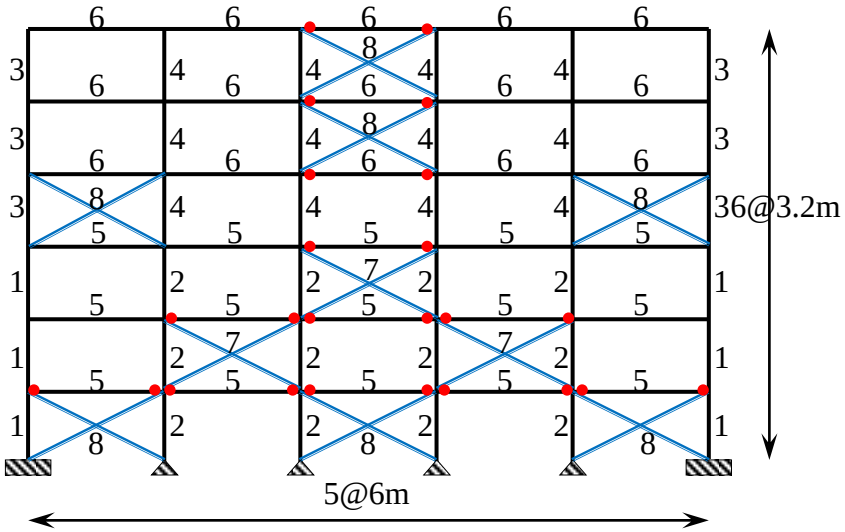

Figure 5. Optimized configuration of X-bracings and connections for six-story frame

6.3 Nine-story frame

Fig. 10 and 11 show optimization convergence history and optimized configuration of X-bracings and connections for nine–story frame, respectively. Table 2 shows list of the sections and resulted structural weight for nine-story frame and compares them with the results for dual system and building frame system [8]. It can be seen that the resulted

structural weights at the present research are lower than those of dual and building frame systems. Figs. 12 and 13 show distribution of inter story drifts considering the bracing layout at different performance levels and pushover diagram for the frame, respectively. The results show that inter-story drifts at the IO performance level is controlling the design and its values are far from the allowable values at the LS and CP performance levels

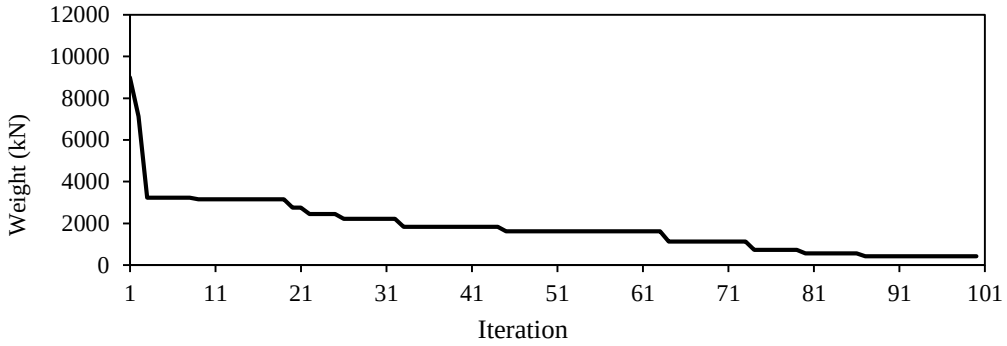

Figure 6. Optimization convergence history of six-story frame

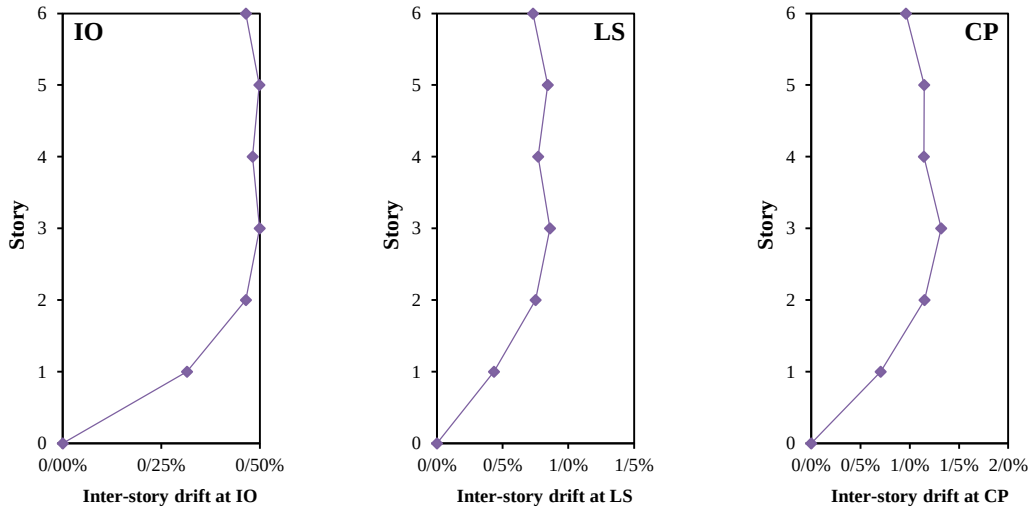

Figure 7. Six-story frame inter-story drifts at different performance levels

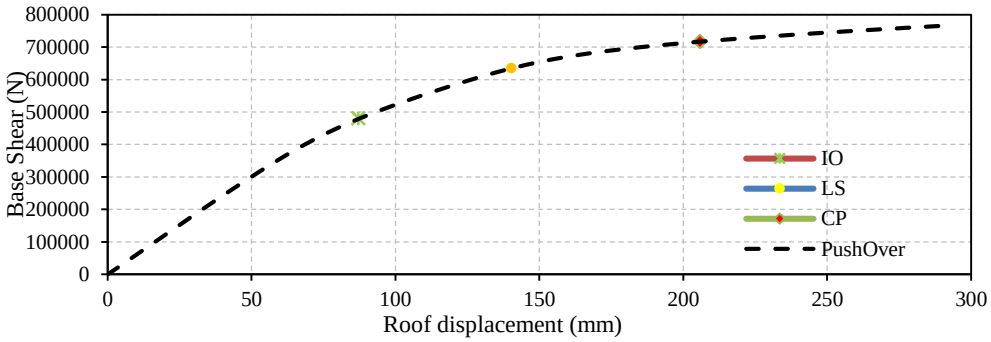

Figure 8. Pushover curve for six-story frame

Table 1: Comparison between results for six-story frame

Members category	Dual system [8]	Building frame system [8]	Present research
1	W24×55	W21×48	W12×96
2	W30×116	W30×90	W40×167
3	W16×40	W14×30	W14×38
4	W16×45	W24×62	W21×44
5	W12×45	W8×35	W10×60
6	W12×58	W14×61	W21×57
7	W10×77	W16×89	W12×30
8	W18×40	W18×50	W8×28
Weight of structure (kN)	432.3	436.7	426.38

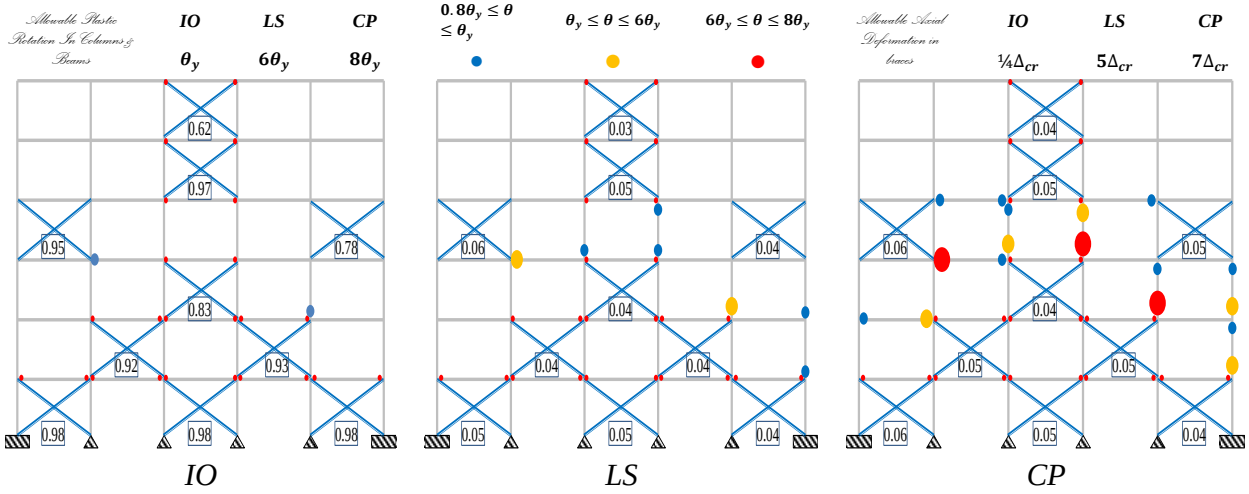

Figure 9. Distribution of plastic rotations and axial displacement ratios of X-bracings at different performance levels for six-story frame

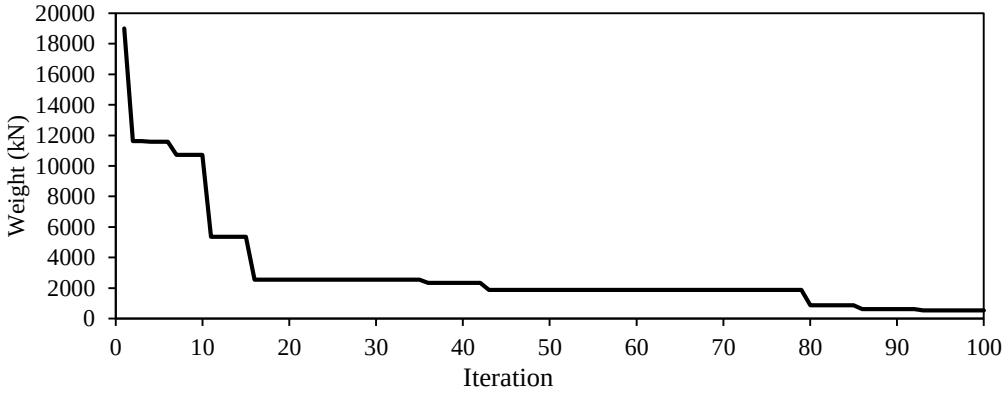

Figure 10. Optimization convergence history for nine-story frame

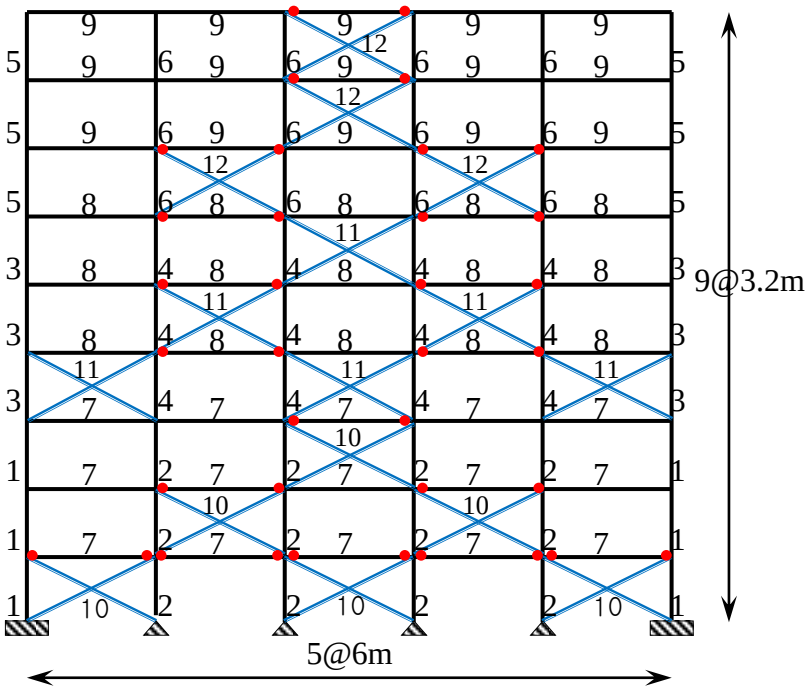

Figure 11. Optimized configuration of X-bracings and connections for nine-story frame

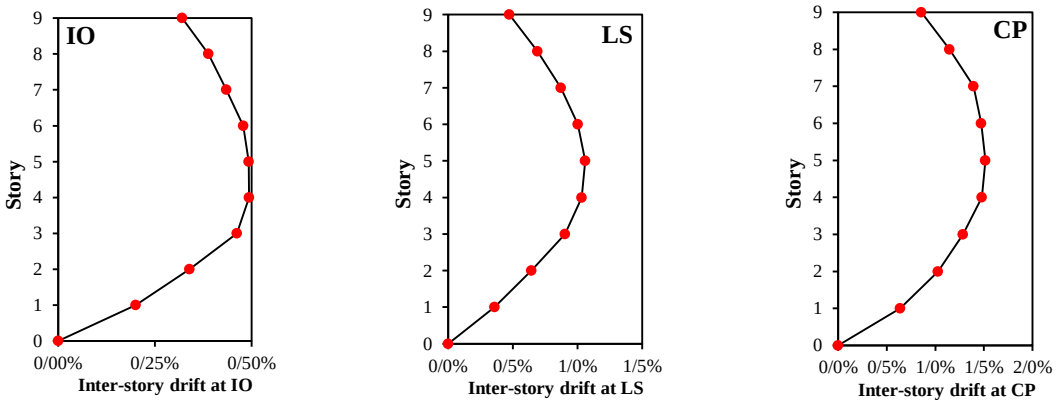

Figure 12. Distribution of inter-story drifts for nine-story frame

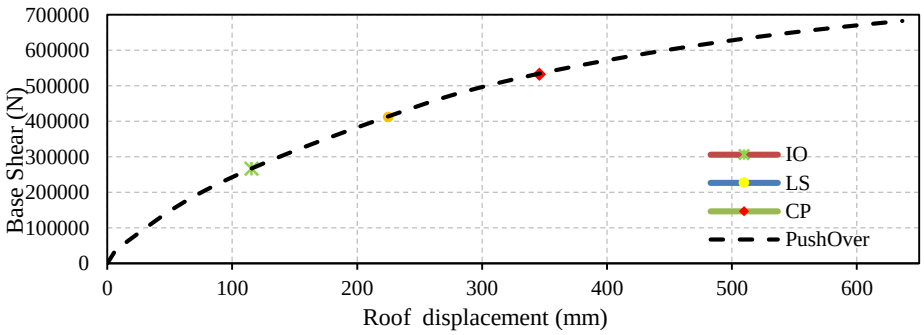

Figure 13. Pushover curve for nine-story frame

Fig. 14 shows the response of the structure at different performance levels, critical design constraints at the IO performance level, axial displacements of the X-bracings, and inter-story drifts. The plastic rotation of the members at the CP performance level is critical because of high deformation.

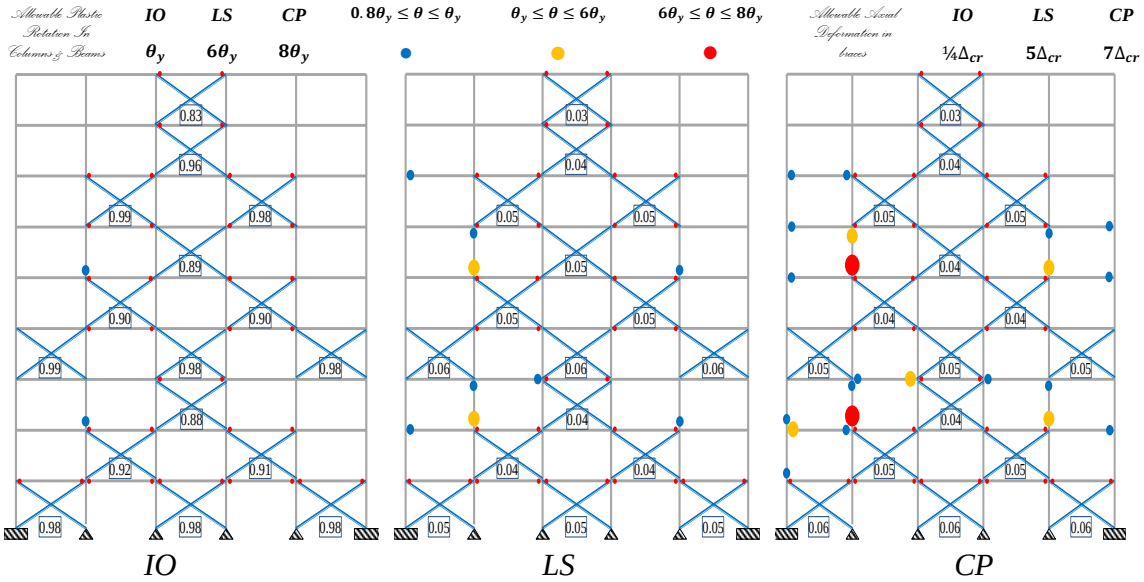

Figure 14. Distribution of plastic rotations and axial displacement ratios of X-bracings at different performance levels for nine-story frame

Table 2: Comparison between results for nine-story frame

Members category	Dual system [8]	Building frame system [8]	Present research
1	W24×76	W27×84	W10×77
2	W27×84	W30×99	W24×103
3	W21×55	W24×62	W24×62
4	W30×90	W12×58	W12×96
5	W14×30	W24×62	W21×48
6	W21×48	W14×34	W18×46
7	W8×31	W8×40	W18×40
8	W18×50	W14×48	W8×40
9	W8×31	W24×62	W10×33
10	W12×53	W16×77	W8×24
11	W10×39	W21×57	W6×25
12	W8×24	W14×26	W10×26
Structure Weight (kN)	559.24	634.28	539.81

6.4 Twelve-story frame

Figs. 15 and 16 show optimization convergence history and optimized configuration of X-bracings and connections for twelve-story frame, respectively.Table 3 shows the list of sections and structures weight for twelve-story frame and compares the results with those of dual and building frame systems [8]. As can be seen, the resulted weights are lower in comparison with dual and building frame systems. Figs. 17 and 18 show distribution of inter story drifts considering the bracing layout at different performance levels and pushover diagram for the frame, respectively. As shown, drift values at IO performance level are controlling the design and their values at LS and CP performance levels are so far from the allowable values.

Fig. 19 shows the structure response at different performance levels, the most critical design constraints at the IO performance level, axial displacement of X-bracings, and inter-story drifts. The plastic rotation of the members is critical at the CP performance level because of increasing structure displacements.

Table 3: Comparison between results for twelve-story frame

Members category	Dual system [8]	Building frame system [8]	Present research
1	W24×76	W44×230	W24×68
2	W33×118	W44×262	W33×201
3	W21×73	W21×182	W21×83
4	W30×90	W33×201	W30×124
5	W16×57	W40×183	W16×45
6	W18×50	W30×90	W18×40
7	W12×26	W36×160	W12×58
8	W8×28	W12×58	W8×40
9	W14×22	W16×89	W14×38
10	W10×49	W8×67	W10×54
11	W16×26	W18×97	W16×45
12	W12×35	W12×79	W12×45
13	W21×83	W30×116	W21×44
14	W12×96	W16×100	W12×58
15	W14×43	W10×88	W14×26
16	W10×22	W14×48	W8×24
Structure weight (kN)	732.96	774.98	708.52

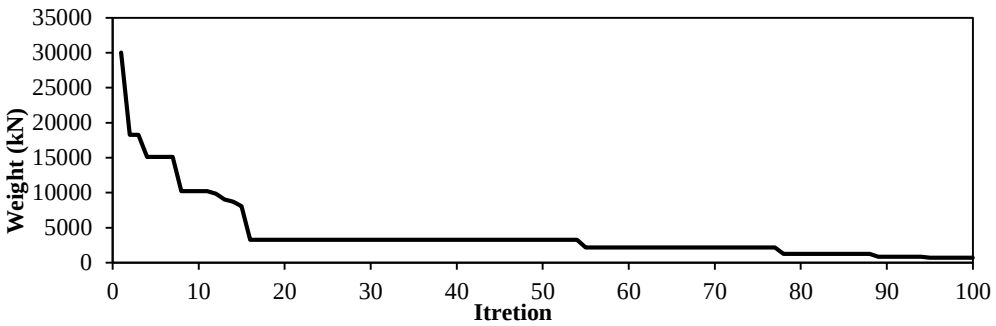

Figure 15. Optimization convergence history for twelve story frame

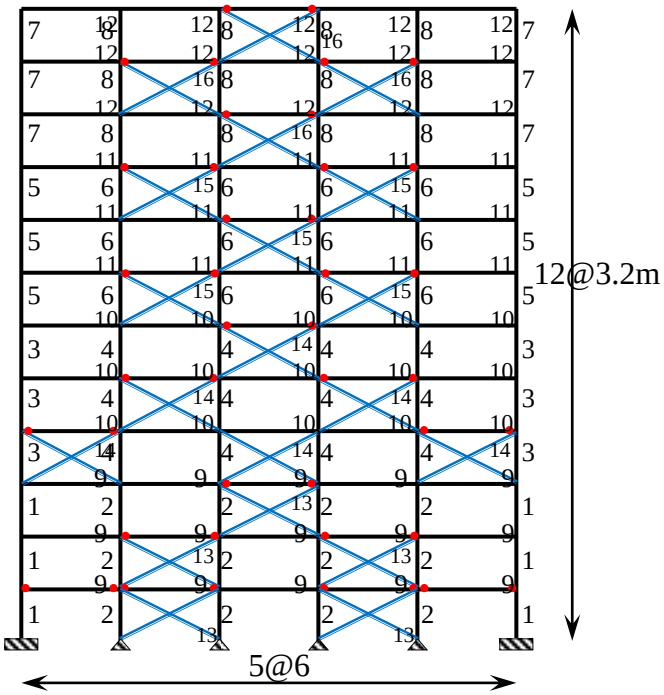

Figure 16. Optimized X-bracings and connections configuration for twelve-story frame

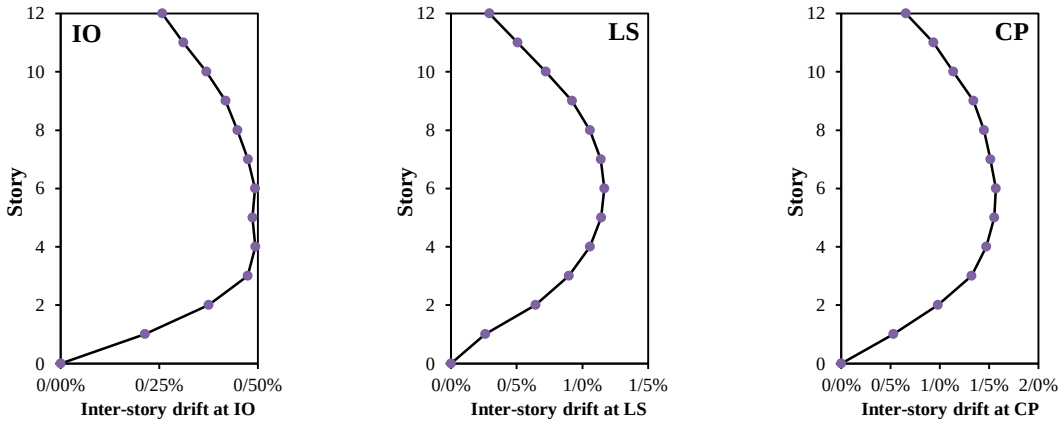

Figure 17. Distribution of inter-story drifts for twelve-story frame

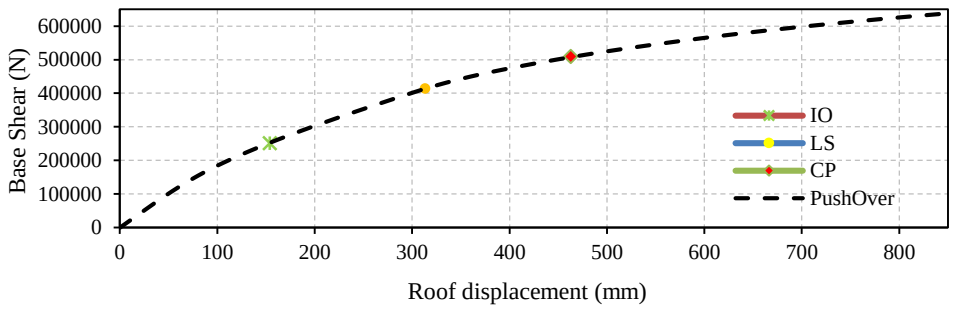

Figure 18. Pushover curve for twelve-story frame

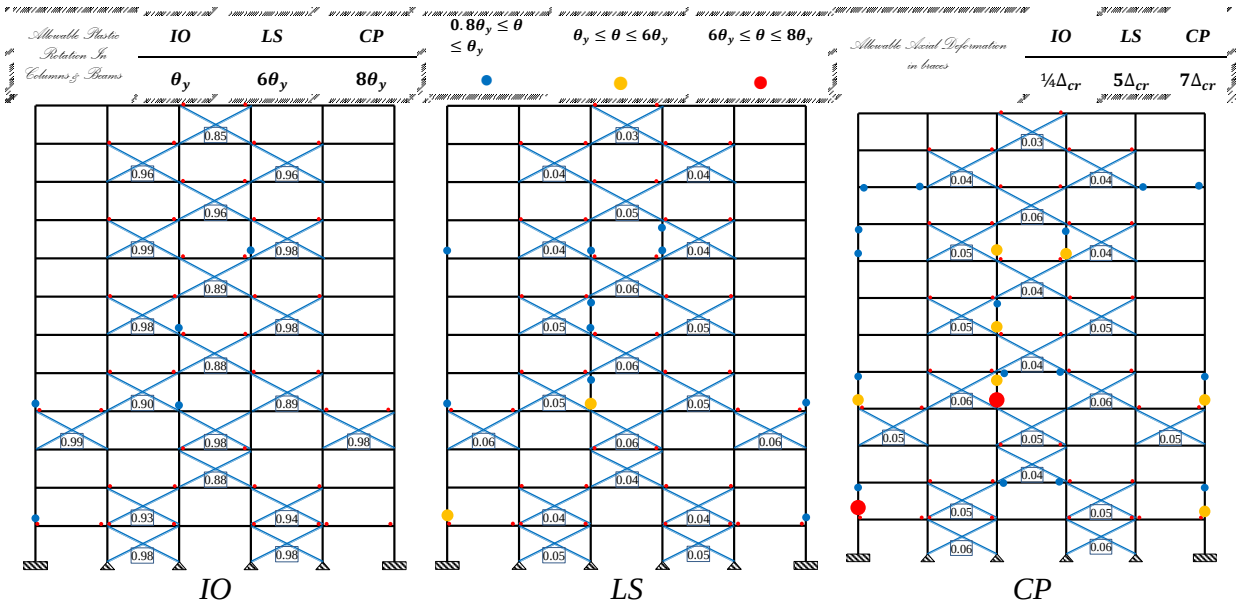

Figure 19. Distribution of plastic rotations and axial displacement ratios of X-bracings at different performance levels for twelve-story frame

7. CONCLUSIONS

Steel braced frames were optimized using FDA at the present research. The type of structure connections were introduced and employed in the optimization method of frame configuration. This new introduction featured the effect of design constraints and led to decreasing the weight of the structures. As shown, the weight of dual systems is usually lower than that of the braced frames. However, the cost of rigid connections for dual systems is greater than that of joint connections for braced frames. It was shown that using appropriate number and location of rigid connections and bracings configuration leads to an optimized design and lower amount of structures weight. The parameters such as possibility of using other types of bracings singly and in combination with other types, the cost of connections, performance in bigger structures, the effect of semi-rigid connections, and cost of structure life cycle can be considered for future studies.

REFERENCES

1. Feng TT, Arora J, Haug Jr E. Optimal structural design under dynamic loads, *Int J Numer Meth Eng* 1977; **11**(1): 39-52.
2. Zou XK, Chan CM, Li G, Wang Q. Multiobjective optimization for performance-based design of reinforced concrete frames, *J Struct Eng* 2007; **133**.
3. SEAOC, Vision 2000, in Performance based seismic engineering of buildings, Structural Engineers Association of California: Sacremento (CA), 1995.

4. James LB, Costas P, Eduardo Ch, Ayhan I. A performance-based optimal structural design methodology, California Institute of Technoloy Pasadena, California, 1997
5. Ganzerli S, Pantelides CP, Reaveley LD. Performance-based design using structural optimization, *Earthq Eng Struct Dyn* 2000; **29**(11): 1677-90.
6. FEMA-356. *Prestandard and Commentary for the Seismic Rehabilitation of Buildings*, 2000, Federal Emergency Management Agency: Washington.
7. Zou XK, Chan CM. Optimal seismic performance-based design of reinforced concrete buildings using nonlinear pushover analysis, *Eng Struct* 2005; **27**(8): 1289-1302.
8. Gholizadeh S, Poorhoseini H. Seismic layout optimization of steel braced frames by an improved dolphin echolocation algorithm, *Struct Multidisc Optim* 2016; **54**(4): 1011-29.
9. Kaveh A, Farhoudi N. A unified approach to parameter selection in meta-heuristic algorithms for layout optimization, *J Construct Steel Res* 2011; **67**(10): 1453-62.
10. Hagishita T, Ohsaki M. Optimal placement of braces for steel frames with semi-rigid joints by scatter search, *Comput Struct* 2008; **86**(21-22): 1983-93.
11. Farzampour A, Khatibinia M, Mansouri I. *Shape optimization of butterfly-shaped shear links using grey wolf algorithm*, 2019.
12. Mansouri I, Soori S, Amraie H, Wan Hu J, Shahbazi Sh. Performance based design optimum of CBFs using bee colony algorithm, *Steel Compos Struct* 2018; **27**(5): 613-22.
13. Mirzai NM, Zahrai SM, Bozorgi F. Proposing optimum parameters of TMDs using GSA and PSO algorithms for drift reduction and uniformity, *Struct Eng Mech* 2017; **63**(2): 147-60.
14. Terazawa Y, Takeuchi T. Optimal damper design strategy for braced structures based on generalized response spectrum analysis, *Japan Architect Rev* 2019; **2**(4): 477-93.
15. Kaveh A, Hoseini Vaez SR, Hosseini P, Ezzati E. Layout optimization of planar braced frames using modified dolphin monitoring operator, *Period Polytech Civil Eng* 2018; **62**(3): 717-31.
16. Danesh M. Evaluation of Siesmic Performance of PBD Optimized Steel Moment Frames by Means of Neural Network, *Jordan J Civil Eng* 2019; **13**(3): 472-88.
17. Ravindra MK, Galambos TV. Load and resistance factor design for steel, *J Struct Div* 1978; **104**(9): 1337-53.
18. Sullivan TJ, Calvi GM, Priestley MJN, Kowalsky M. The limitations and performances of different displacement based design methods, *J Earthq Eng* 2003; **7**(spec01): 201-41.
19. Pourbaba M, Azimi S. *Practical and Economic Evaluation of Concrete Structures Designed Based on 3rd and 4th Edition Of Iran 2800 CODE*, 2016.
20. Vanderplaats GN. *Numerical Optimization Techniques for Engineering Design*, Vanderplaats Research and Development, Incorporated, 2001
21. Gu Q, Conte J, Barbato M. *OpenSees command Language Manual Response Sensitivity Analysis Based on the Direct Differentiation Method (DDM)*, Berkeley, CA: Pacific Earthquake Engineering Center, University of California, 2010.
22. MathWorks I, *MATLAB: The Language of technical Computing. Desktop Tools and Development Environment, Version 7*. Vol. 9. 2005: MathWorks.
23. Celebi M, Sanli A, Sinclair M, Gallant S, Radulescu D. Real-time seismic monitoring needs of a building owner-and the solution: a cooperative effort, *Earthq Spect* 2004; **20**(2): 333-46.